Investigation of the ion transit time instability in a Hall thruster combining time-resolved LIF spectroscopy and analytical calculations

IEPC-2015-400／ISTS-2015-b-400

Presented at Joint Conference of 30th International Symposium on Space Technology and Science, 34th International Electric Propulsion Conference and 6th Nano-satellite Symposium
Hyogo-Kobe, Japan
July 4–10, 2015

J. Vaudolon* and S. Mazouffre†
CNRS - ICARE (Institut de Combustion, Aerothermique, Reactivite et Environnement)
1C, Avenue de la Recherche Scientifique, 45071 Orleans Cedex 2, France

The performance of Hall thrusters is greatly influenced by the discharge current oscillations. In order to characterize the oscillations of the plasma parameters, we have measured the time-varying Xe^+ ion velocity distribution in the discharge channel and in the near-field plume of a low-power permanent magnets Hall thruster. The distribution functions are obtained by means of a time-resolved laser-induced fluorescence technique based on a photon counting method, while time coherence is ensured by applying a sinusoidal potential modulation on a floating electrode located in the plasma to achieve resonance with the breathing mode. The measurements are therefore local, non invasive and the temporal resolution is 100 ns. The discharge oscillations are consistent with those of a standard operating point. The axial ion dynamics in the [100 kHz;1 MHz] band, i.e. the so-called ion transit time instability, is examined. The high-frequency spectral properties of the ion mean velocity are compared with a perturbed fluid model of the plasma flow on the source axis. The wavelength of the high-frequency axial mode is similar to the electric field extent outside the cavity. Surprisingly the mode appears only in the area of negative magnetic field gradient.

Nomenclature

(r, θ, z)	= cylindrical coordinate system
f	= ion velocity distribution
n	= plasma density
v_z	= ion mean axial velocity
u	= electron velocity
Φ	= accelerating potential
m_i	= Xe^+ ion mass
m_e	= electron mass
e	= elementary charge
B_r	= magnetic field
$\mathbf{k}$	perturbation wave vector
f, ω	= frequency

*PhD candidate, Electric Propulsion Team, julien.vaudolon@cnrs-orleans.fr
†Head of Electric Propulsion Team, stephane.mazouffre@cnrs-orleans.fr

I. Introduction

In the field of space propulsion, the necessity to perform various missions requires versatile thrusters, high reliability and performance. Electric propulsion has the benefit of a low propellant consumption and a significant thrust to power ratio resulting in mass and cost savings compared to chemical propulsion. Plasma propulsion is mostly dedicated to high ΔV manoeuvres such as station keeping and orbit topping for communication satellites. In a very near future, this technology will be used to realize full orbit transfers and interplanetary journeys. Despite decades of research on Hall thrusters, the physics at play is far from being fully understood. Careful experiments are therefore needed by engineers and by numerical simulations for their outcome validation.

Hall thruster plasmas are characterized by a broad family of oscillatory phenomena.[1] Knowledge of the instability characteristics is key for describing plasma processes, such as the anomalous electron transport, ionization, ion acceleration and ultimately the thruster performance. Yet many properties of these oscillations remain poorly-understood.[2] While many experimental and numerical studies have focused on ionization instabilities in the kHz range and on electron turbulence in the MHz range,[3–6] experimental work on the intermediate frequency band instabilities remains rare. While a wide variety of models has been developed, no experimental validation supports their outcomes.[7,8] In Hall thrusters, this intermediate range of oscillations between 100 kHz and 1 MHz is oft-referred to as the ion transit-time (ITT) instability, because the typical time period is on the order of the ion time-of-flight through the acceleration region. The practical difficulty of accessing the ion dynamics over a very short time scale, without perturbing the plasma, has made knowledge of the fundamental properties of the ITT difficult to obtain.

Examination of the instable behavior of the discharge requires a tailored diagnostic instrumentation. The present paper reports the first direct evidence of the ITT instability in a low-power Hall thruster in a non-invasive manner, by means of time-resolved laser-induced fluorescence (TR-LIF) measurements of the ion velocity distribution function (IVDF). The measurements, associated with a two-fluid model of the plasma, reveal complex physics which depends on the low frequency ionization mode and the magnetic field profile. The experiments have been carried out in the discharge of a 200 W permanent magnets Hall thruster at a constant discharge voltage of 200 V and an anode mass flow rate of 1.0 mg/s.[9] The so-called $2S_0$ geometry has been used (the channel width is increased twice compared to a standard design) with BN-SiO_2 channel walls. The background pressure has been kept under 7.10^{-5} mbar-N_2 during operation. The discharge current fluctuations are consistent with those of a Hall thruster operating under standard flight conditions. The discharge voltage is 200 V. Xe has been used as a working gas. The cathode mass flow rate is 0.2 mg/s. The source is electrically floating, which mimics the flight mode operation. Axial IVDFs, $f(\mathbf{x}, v_z, t)$, have been recorded along the source channel axis, from -13 mm up to 10 mm, where the position 0 mm is the channel exit plane. Due to the annular geometry of the source, we use a (r, θ, z) cylindrical coordinate system.

The TR-LIF diagnostic and the discharge modulation techniques are presented in Sec. II. The particular signal processing method that has been employed is described. The ion oscillations at a few hundreds of kHz are examined in Sec. III. A novel insight on the ion transit time instability triggering mechanism is gained. Finally, concluding remarks are drawn in Sec IV.

II. Diagnostic technique

A. Optical bench and collection branch

The LIF optical assembly is described in details in a review paper.[10] The $5d^2F_{7/2} \rightarrow 6p^2D_{5/2}$ transition of the Xe^+ ion is probed by an amplified tunable single-mode external cavity laser diode at 834.72 nm. The wavelength is accurately measured by a calibrated 60 m/s precision wave meter. A high finesse Fabry-Perot interferometer is used to check the laser stability and detect mode-hops. A pair of anamorphic prisms circularize the laser beam and maximize the transmission through the optical fiber. The laser beam propagates along the thruster axis and is aligned with the center of the discharge channel. The laser typical power density is 10 mW/mm^2 within the measurement volume, which warrants a good signal-to-noise ratio and a limited saturation of the transition. A collection branch made of a 40 mm focal lens focuses the light onto a 200 µm core diameter optical fiber. The magnification ratio is 1, meaning spatial resolution in the axial direction is 200 µm. The fluorescence light is focused onto the entrance slit of a 20 cm focal length monochromator that isolates the 541.9 nm line from the background light.

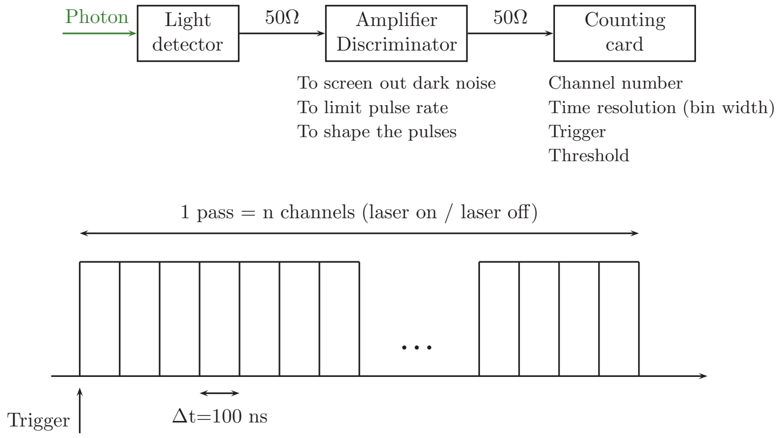

Figure 1. Schematic of the detection branch. Photon events are amplified and selected depending on their energies. The counting card accumulates the events over n channels of 100 ns length each. Both laser-on and laser-off acquisitions are performed to screen out the noise and reveal the fluorescence.

B. Photon-counting technique

The photon counting technique has been applied in the past to diagnose oscillating and pulsed discharges.[11,12] However, this is the first time this technique is applied to the remotely-stabilized plasma of a Hall thruster. The detection branch is sketched in Fig. 1. Photons are detected by means of a high gain low dark noise Hamamatsu R7518P photomultiplier tube. A fast amplifier and discriminator 9302 module from Ortec is used to screen out the noise from the PMT. This has two advantages. Firstly, the count rate is limited to avoid the pulse counter saturation. Secondly, any incoming photon is converted into a TTL signal. Each photon pulse can be distinguished from the background noise by an appropriate setting of the discriminator threshold.

The pulses are counted by a MCS-PCI multichannel scaler from Ortec, composed of 65,535 channels. The saturation occurs for pulse trains whose frequency exceeds 150 MHz. The direct observation of the discriminator output pulse train by an oscilloscope has made it possible to estimate the count rate to about 10 MHz during our experiments. The modulation signal acts as a trigger which starts the counting of the incoming photon events over a few oscillations period, which warrants perfect reproducibility for each pass. The channel width (the temporal resolution) is 100 ns. Hundreds of thousands of passes are necessary to obtain a suitable LIF signal-to-noise ratio. The laser wavelength is kept constant through a feedback loop, the uncertainty being that of the wavemeter. The fluorescence signal (typically a hundred photons per minute) is extracted by subtracting laser off measurements from laser on acquisitions. As highlighted earlier, the entire period of the oscillation can be recorded instead of being reconstructed by an external device over several oscillation periods. Additionally, any wave shape can be recorded with this technique.

C. Active control method of the discharge oscillations

At low-pressure, i.e. in low density discharges like Hall thrusters, the recorded fluorescence signal consists of just a few photons per oscillation period. Even if the number of fluorescence light events can be increased by working in a strongly saturated regime, it appears necessary to realize a statistical accumulation. A temporal coherence of the oscillations is therefore required to perform such an accumulation.

In order to achieve TR-LIF in a Hall thruster, the discharge needs to be maintained in a periodic oscillation regime. The active harmonic system presented here has two main advantages: firstly, the modulation signal can be used as a trigger signal. Secondly, the frequency content is fairly the same at any time, which warrants reproducible measurement conditions. Another possibility to actively perform TR-LIF is to use a fast power switch. However, it has been shown that unlike the technique presented here, the power switch perturbs the discharge behavior.[13] Passive systems such as phase sensitive detection time-synchronized on a particular level of the discharge current have been used to extract time-resolved fluorescence signal.[14] This

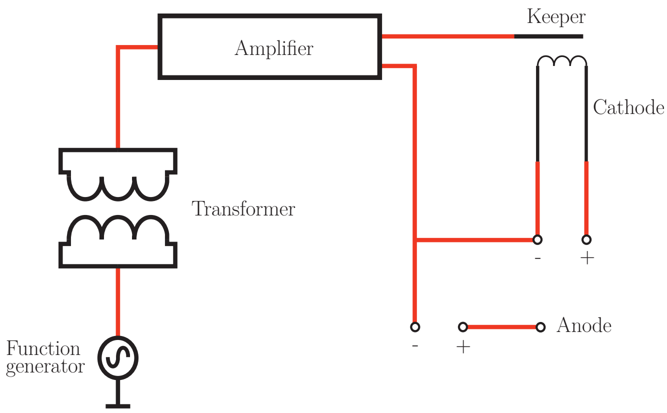

Figure 2. Electrical set-up of the keeper modulation.

method, as well as the one described in this work (photon counting), is not dependent upon the frequency of the recorded signal and can therefore be applied to many situations. However our stabilizing technique warrants a constant frequency content during operation. Such conditions cannot be obtained through a passive detection.
In order to control the oscillations, a sinusoidal frequency-tunable potential is applied between a floating electrode in the vicinity of the cathode (referred to as the keeper) and the negative pole of the cathode. A schematic view is presented in Fig. 2. The modulation frequency cannot be chosen randomly but corresponds to a resonance of the system. The discharge current oscillation amplitude is monitored as the frequency is adjusted in order to maximize the plasma response to the excitation. The current driven through the keeper is relatively small and represents approximately 6% of the discharge current. The potential stimulation peak-to-peak amplitude equals 120 V. Such a modulation has been used in the past to perform probe measurements in the far-field plume of Hall thrusters.[15]

The resonance with the breathing mode occurs over a 2 kHz band. The monitoring of the maximum discharge current amplitude enables to properly calibrate the modulation frequency. Figure 3 shows the effect of the modulation system on the discharge current. The modulation is set to 16.5 kHz. Firstly it is clear that the mean value of the discharge current remains unchanged, which is mandatory to keep the same thruster average behavior. Secondly, the discharge current amplitude is clearly higher with the modulation. Although it does not appear on a single screenshot, the ensemble averaging over multiple acquisitions shows a constant time-averaged amplitude. Thirdly, the discharge current phase is constant, which ensures temporal coherence between each measurement pass. The frequency content of the discharge is given by its FFT. The same harmonic structures exist with and without the modulation except at a particular frequency which corresponds to the modulation. It is worth noting that the spectral power density remains unchanged elsewhere. The average modulated discharge current frequency is equal to that of the modulation. The same evolution of the cathode potential relative to the ground has been observed. The capability of modulating the discharge is related to the ratio of the input power of the modulation amplifier to the power of the system to be modulated. A value of 5% enables efficient control and does not disturb the thruster average behavior. A similar modulation system has been successfully built and tested on a 1.5 kW Hall thruster. In order to achieve proper control upon the breathing mode, a higher amplification was necessary in this case. Similar characteristics of the plasma parameters were observed, meaning this technique is sizeable.

D. Post-processing technique

The Hilbert-Huang spectral analysis has been applied to the measured time series.[16,17] Unlike Fourier transform, this technique is well-suited for the study of non-stationary and non-linear signals. Based on Huang's sifting algorithm, the Hilbert spectral method allows the computation of the Hilbert and frequency spectra of a signal. The frequency spectrum is called a *marginal spectrum* in the Hilbert spectral domain.[16,17] This spectrum is somewhat similar to a Fourier spectrum, with the additional contribution of the time-dependent nature of the frequency content.

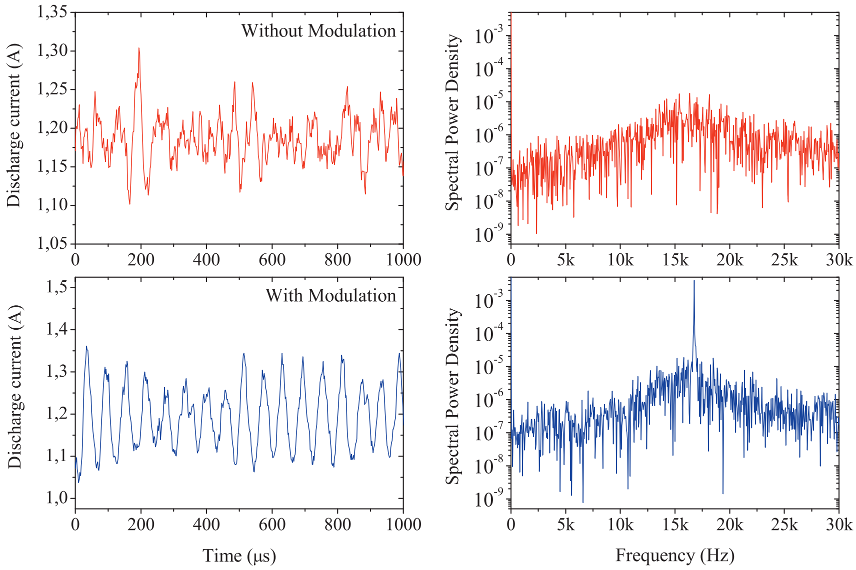

Figure 3. Impact of the potential modulation on the discharge current waveforms. A peak response of the plasma has been reached at a modulation frequency of 16.5 kHz.

The spectral analysis outcome is exemplified in Fig. 4. The marginal spectrum of the ion mean velocity at 1 mm downstream the source exit plane is shown. The marginal spectrum reveals three distinct regimes. The breathing mode contains the main part of the energy at 10-20 kHz. Two other oscillating regimes are located at 100 kHz and 575 kHz. The Hilbert spectrum of the latter oscillation is shown in the figure bottom. The intermittent nature of this regime is clearly seen, and justifies the application of the Hilbert-Huang technique. Structures that contain a significant amount of energy are observed above 100 kHz while the time coherence is based on stabilizing a low frequency mode of the discharge at $\sim$ 15 kHz. Whether the link between the low and high frequency oscillations happens naturally in Hall thrusters, or is influenced by the oscillatory driving of the discharge remains unknown though. The results of Fig. 4, and examples of coherent structures obtained through the Hilbert-Huang analysis that can be found in Ref.,[18] show that the ion dynamics in the [100 kHz;1 MHz] band is either controlled and stabilized by the breathing mode, or influenced by the modulation apparatus.

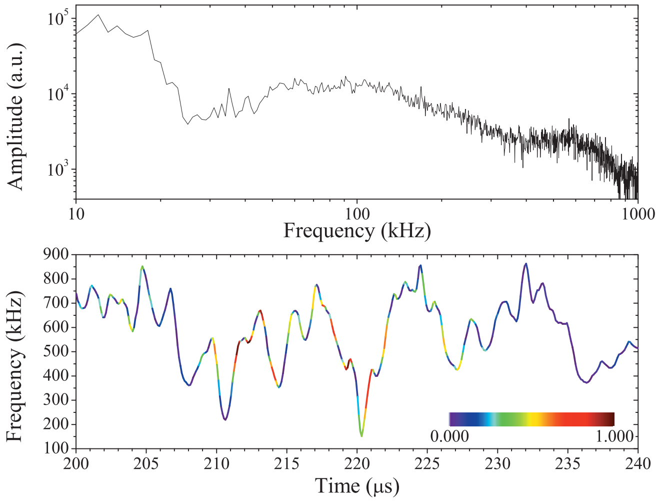

Figure 4. Marginal and Hilbert spectra of the ion mean velocity oscillation at z=1 mm: (top) marginal spectrum ; (bottom) oscillation at 575 kHz. The colorbar indicates the normalized power level.

III. Results and discussion

A. Time-varying ion velocity distribution

The IVDF obtained at 4 mm downstream the thruster exit plane is represented in Fig. 5 for illustrating the measurement outcome. The frequency content above 1 MHz have been removed from the raw data. The number of fluorescence photons is presented as a function of both the ion velocity and time during three breathing oscillations. The number of photons of the most probable velocity group at 11 km/s is phased with the discharge current waveform,[18] meaning that the low-velocity tail of the distribution is periodically populated during the replenishment of the channel by neutral species.[5] Charge-exchange collisions or the back-and-forth movement of the ionization area can be invoked to explain the presence of slow ions. Typical charge-exchange cross sections for singly-charged xenon ions lies around 6.10^{-17} m^2, and neutral density close to 10^{18} m^{-3}, which make the mean free path on the order of 2 cm. Therefore, it seems quite unlikely that this group originate from CEX collisions.

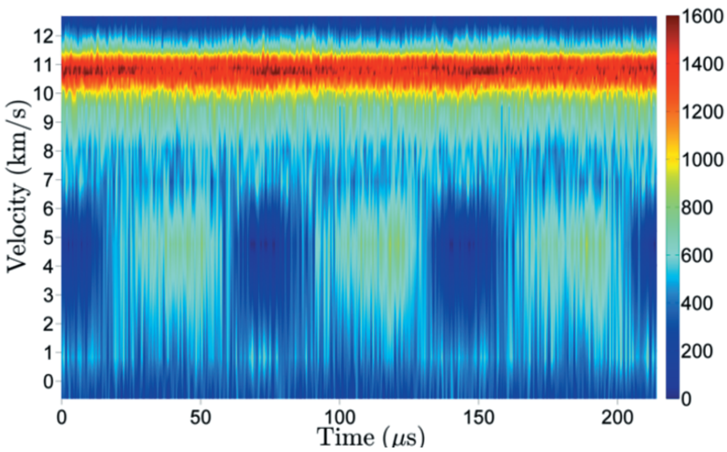

Figure 5. Axial ion velocity distribution at 4 mm away from the discharge channel as a function of time. The window spans 3 breathing oscillations. The colorbar represents the number of fluorescence photons. Low-velocity ions are created during the replenishment of the channel by neutrals.

Several oscillation regimes can be observed in Fig. 5, notably the low frequency ionization mode, which is relatively narrow-band, and a superposition of high-frequency oscillations that cannot be precisely characterized in the present form. The marginal spectra of four velocity groups are presented in Fig. 6. The corresponding ion velocity is indicated within the frame of each plot. The general trend in amplitude is similar, i.e. the breathing mode is carrying most of the energy and one or two oscillations are observed at higher frequencies. The breathing mode amplitude for the low-velocity group at 4.8 km/s is much higher than that of the others, which is perceptible in Fig. 5. Similarly to the observation in Fig. 4, coherent oscillating patterns are observed at frequencies much above the breathing mode, and suggest a transfer of energy between the various modes, or directly from the modulation apparatus.

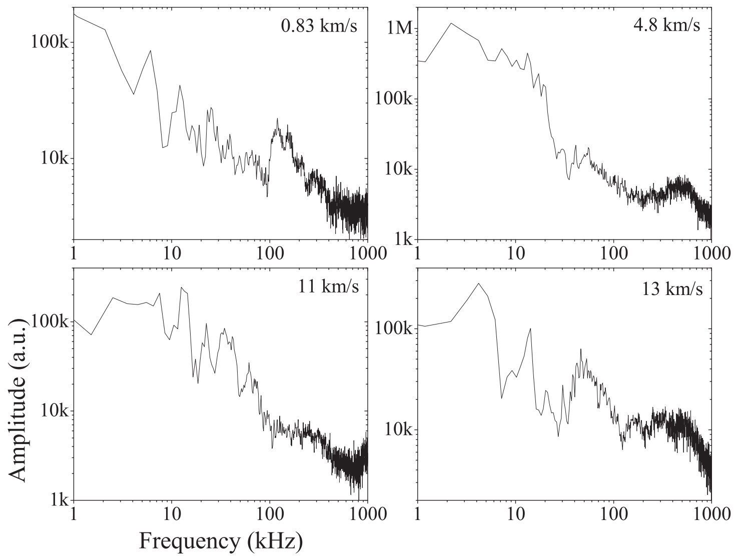

Figure 6. Marginal spectra of the axial IVDF at 4 mm downstream the exit plane. Oscillations with frequencies ranging far above the breathing mode can be observed.

B. Investigation of the ion transit time instability

While the low frequency oscillations are well-understood, the transit time instability description has not progressed much from an experimental viewpoint since the early work of Esipchuk and Morozov in 1973,[19] rendering the comparison with fluid models impossible. Observations of the floating plasma potential reported at that time an instability, occurring at a frequency corresponding to the reciprocal ion time-of-flight through the acceleration zone, $f \approx v_z/L$, with a wide spread in frequency so that $\Delta f \approx f$.

The marginal spectrum of the time-resolved ion mean velocity (first order moment of the IVDF) has been computed at each measurement location, which allows to detect the existence of the instability, and ultimately to compute its frequency content. In order to extract more information from the measured IVDF, we correlate the experimental observations to a linearised one-dimensional two-fluid model of the plasma, and determine the plasma parameters which influence the instability.

The plasma is assumed to be composed of cold unmagnetized ions and cold magnetized electrons. The magnetic field is assumed to be purely radial, which is a reasonable approximation on the cavity axis. We study the case of quasineutral perturbations, and dissipative and ionization processes are neglected. For the sake of simplicity, and for allowing the comparison of the theoretical results with the LIF data set, the model is one-dimensional. The electric field profile along the chamber axis has been obtained using the LIF measurements and a fluid computation.[20] Finally, we consider that the typical transit time frequency ω is much lower than the electron cyclotron frequency ω_{Be}, so that $\omega << \omega_{Be}$. Under these assumptions, the continuity equation and the momentum conservation equation for both the ions and the electrons are linearised and read

$$
\begin{cases}
\dfrac{\partial \tilde{n}}{\partial t} + n\dfrac{\partial \tilde{v}_z}{\partial z} + v_z\dfrac{\partial \tilde{n}}{\partial z} + \tilde{v}_z\dfrac{\partial n}{\partial z} + \tilde{n}\dfrac{\partial v_z}{\partial z} = 0,\\
\dfrac{\partial \tilde{v}_z}{\partial t} + v_z\dfrac{\partial \tilde{v}_z}{\partial z} + \tilde{v}_z\dfrac{\partial v_z}{\partial z} = -\dfrac{e}{m_i}\dfrac{\partial \tilde{\Phi}}{\partial z},\\
\dfrac{\partial \tilde{n}}{\partial t} + n\dfrac{\partial \tilde{u}_z}{\partial z} + \tilde{u}_z\dfrac{\partial n}{\partial z} = 0,\\
\dfrac{\partial \tilde{u}_\theta}{\partial t} = \dfrac{e}{m_e}\tilde{u}_z B_r,\\
\dfrac{\partial \tilde{u}_z}{\partial t} = \dfrac{e}{m_e}\left(\dfrac{\partial \tilde{\Phi}}{\partial z} - \tilde{u}_\theta B_r\right),
\end{cases}
\tag{1}
$$

where the subscripts r, θ and z refer to the cylindrical coordinates, v and u are the ion and electron velocities respectively, n is the plasma density, Φ the accelerating potential, e the ion charge, m_i the ion mass, m_e the electron mass and B_r the magnetic field. Perturbed quantities are labelled by a tilde superscript. We look for the solution of system (1) in Fourier form $\exp\left[i\left(kz - \omega t\right)\right]$ where $\mathbf{k} = (0, 0, k)$ is the perturbation wave-vector.
After a few manipulations, the dispersion relation is obtained in the form of (2), in which ω_{Bi} is the ion cyclotron frequency. Equation (2) has two complex roots. Only one of them has a positive real part and is therefore considered as the physical solution. The solution of the dispersion relation is given by (3). In the remaining of the analysis, we write $\omega = \omega_r + i\gamma$ where ω_r is the mode frequency and γ is the growth rate of the instability.

$$
\left(\frac{1}{v_z}\frac{\partial v_z}{\partial z} + \frac{2}{B_r}\frac{\partial B_r}{\partial z} - ik\right)\left(\frac{1}{v_z}\left[i\omega - \frac{\partial v_z}{\partial z}\right] - ik\right)^2 + \frac{\omega_{Be}\omega_{Bi}}{v_z^2}\left(\frac{1}{v_z}\frac{\partial v_z}{\partial z} - ik\right) = 0. \tag{2}
$$

$$
\omega = v_z k - i\left\{\frac{\partial v_z}{\partial z} + \left[\frac{\omega_{Be}\omega_{Bi}\left(ik - \frac{1}{v_z}\frac{\partial v_z}{\partial z}\right)}{\frac{1}{v_z}\frac{\partial v_z}{\partial z} + \frac{2}{B_r}\frac{\partial B_r}{\partial z} - ik}\right]^{\frac{1}{2}}\right\}. \tag{3}
$$

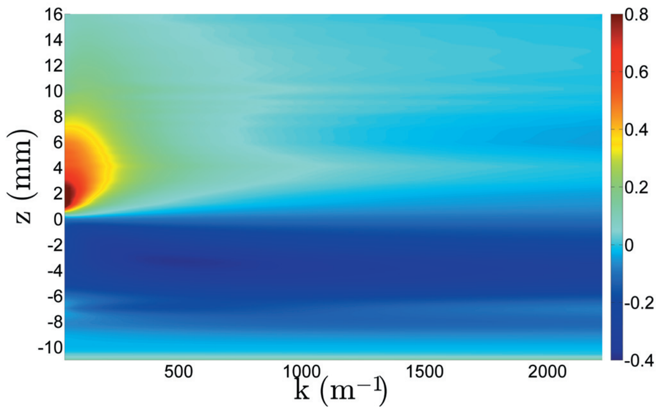

Figure 7. Growth rate mapping as a function of the mode wavenumber and axial position along the cavity axis. The colorbar is expressed in MHz.

The growth rate of the instability is mapped in Fig. 7, in MHz, as a function of the mode wavenumber and axial position along the cavity axis. Regions in which the growth rate is positive, and where unstable modes are therefore likely to appear, extend downstream the source exit plane, for $z > 1$ mm and $k < 1000$ m^{-1}. The corresponding wavelength is on the order of the width of the electric field distribution outside the cavity.

The growth rate becomes negative for higher wavenumbers between $z = 4$ to 9 mm, which is the location of the high electric field region. Details concerning the electric field distribution in this source can be found in Ref.[18] It is worth noting that the growth rate is negative for any wavenumber in regions where $z < 1$ mm, i.e. inside the cavity. Expanding the dispersion relation and factorizing by the powers of γ, it can be seen that, in our operating conditions, the sign of the growth rate is determined by the opposite sign of $\frac{\partial v_z}{\partial z} + 2\frac{v_z}{B_r}\frac{\partial B_r}{\partial z}$. Owing to the strong axial electric field, $\frac{\partial v_z}{\partial z} > 0$ at each location, and therefore the instability triggering is primarily determined by the magnetic field profile.

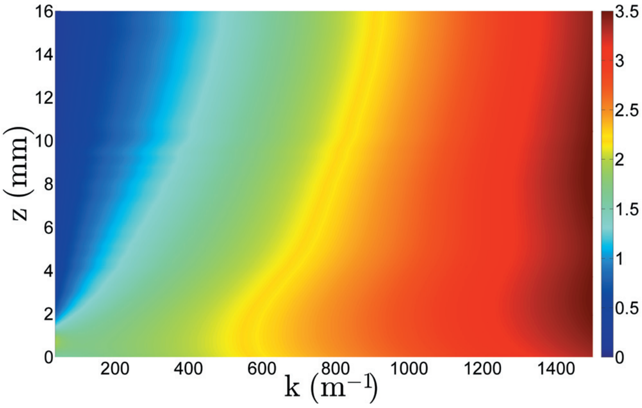

Figure 8. Colormap of the mode frequency as a function of wavenumber and axial location. The colorbar is expressed in MHz**.**

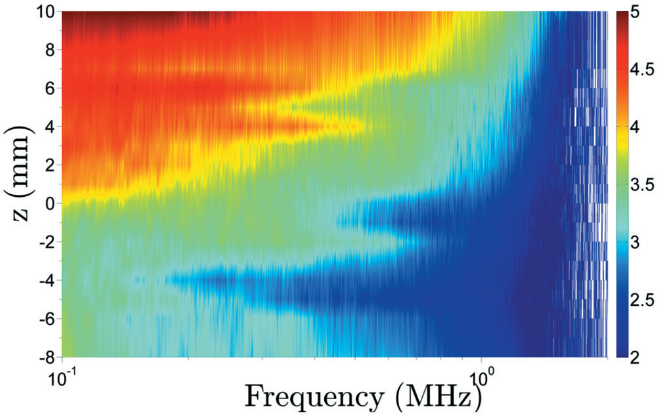

Figure 9. Experimental marginal spectra of the ion mean velocity as a function of z. The colorbar is expressed in arbitrary units.

The mode frequencies are mapped in Fig. 8, in MHz, in the area of positive growth rate, as a function of the mode wavenumber and axial position along the cavity axis. The instability is more likely to occur at low wavenumbers, which scale with the acceleration zone length, on the order of 1 cm. In this region, frequencies range from 150 kHz to 1.2 MHz, which is on the order of magnitude of the reciprocal ion time-of-flight through the device $\approx v_z/L$.

The experimental marginal spectra of the ion mean velocity temporal evolution are presented in Fig. 9, as a function of the axial position along the cavity axis. The colorbar is expressed in arbitrary units. Agreement can be found between the experimental results and the analytical results. The order of magnitude of the mode frequency indeed appears to be similar, ranging in the 100 kHz-1.1 MHz band. Notice that the experimental results confirm the turbulent nature of the instability first reported by Esipchuk and Morozov,[19] i.e. the frequency spread is on the same order of magnitude as the frequency scale: $\Delta f \approx f$. A noticeable feature can be found in Fig. 9. The amplitude of the unstable mode increases rapidly outside the cavity. This picture is in agreement with the growth rate profile analyzed previously, which indicates that the magnetic field profile may indeed be a key element for describing the instability occurrence.

IV. Conclusion

The first experimental description of the high frequency ion dynamics in a Hall thruster with high spatial and temporal resolution has been reported. The TR-LIF technique, based on a photon-counting method and active stabilization of the discharge behavior, shows that the high frequency ion properties are influenced by the lower frequency breathing mode, or by the modulation of the keeper electrode. The properties of the ion mean velocity have been compared with a one-dimensional two-fluid model. The ion transit-time oscillation appears only in the region of negative magnetic field gradient both analytically and experimentally. Additionally, its wavelength appears to be similar to the electric field distribution extent outside the cavity.

Acknowledgements

The authors would like to thank S Tsikata for stimulating discussions and T André for his assistance in numerical matters. J Vaudolon benefits from a CNES-Snecma PhD grant.

References

[1]E.Y. Choueiri. Plasma oscillations in Hall thrusters. *Phys. Plasmas*, 8:1411, 2001.

[2]V. V. Zhurin, H. R. Kaufman, and R. S. Robinson. Physics of closed drift thrusters. *Plasma Sources Sci. Technol.*, 8:R1, 1999.

[3]C. L. Ellison, Y. Raitses, N. J. Fisch. Cross-field electron transport induced by a rotating spoke in a cylindrical Hall thruster. *Phys. Plasmas*, 19:013503, 2012.

[4]S Tsikata, C Honoré and D Grésillon. Collective Thomson scattering for studying plasma instabilities in electric thrusters. *Journal of Instrumentation*, 8(10):C10012, 2013.

[5]J. P. Boeuf and L. Garrigues. Low frequency oscillations in a stationary plasma thruster. *J. Appl. Phys.*, 84(7):3541, 1998.

[6]N. Brenning, D. Lundin, T. Minea, C Costin, C. Vitelaru. Spokes and charged particle transport in HiPIMS magnetrons. *J. Phys. D: Appl. Phys.*, 46(084005), 2013.

[7]S Barral, K. Makowski, Z. Peradzyński, M. Dudeck. Transit-time instability in Hall thrusters. *Phys. Plasmas*, 12(073504), 2005.

[8]A. Kapulkin, E. Behar, Y. Raitses. Ion Beam Instability in Hall Thrusters. In Proceedings of the 33rd International Electric Propulsion Conference, Washington, D.C., USA, 2013.

[9]S. Mazouffre, G. Bourgeois, K. Dannenmayer, A. Lejeune. Ionization and acceleration processes in a small, variable channel width, permanent-magnet Hall thruster. *J. Phys. D: Appl. Phys.*, 45(185203), 2012.

[10]S. Mazouffre. Laser-induced fluorescence diagnostics of the cross-field discharge of Hall thrusters. *Plasma Sources Sci. Technol.*, 22(013001), 2013.

[11]B. Pelissier and N. Sadeghi. Time-resolved pulse-counting lock-in detection of laser induced fluorescence in the presence of a strong background emission. *Rev. Sci. Instrum.*, 67(3405), 1996.

[12]D. Gawron S. Mazouffre and N. Sadeghi. A time-resolved LIF study on the ion velocity distribution function in a Hall thruster after a fast current disruption. *Phys. Plasmas*, 16(043504), 2009.

[13]S. Mazouffre, G. Bourgeois. Spatio-temporal characteristics of ion velocity in a Hall thruster discharge. *Plasma Sources Sci. Technol.*, 19(065018), 2010.

[14]M.A. Capelli N.A. MacDonald and W.A. Hargus. Time-synchronized continuous wave laser-induced fluorescence on an oscillatory xenon discharge. *Rev. Sci. Instrum.*, 83(113506), 2012.

[15]M. Tichy K. Dannenmayer, P. Kudrna and S. Mazouffre. Time-resolved measurement of plasma parameters in the far-field plume of a hall effect thruster. *Plasma Sources Sci. Technol.*, 21(055020):9, 2012.

[16]N.E. Huang, Z. Wu. A review on Hilbert-Huang transform: Method and its applications to geophysical studies. *Rev. Geophys.*, 46(RG2006), 2008.

[17]J. Kurzyna, S. Mazouffre, A. Lazurenko, L. Albaréde, G. Bonhomme, K. Makowski, M. Dudeck, Z. Peradzyński. Spectral analysis of Hall-effect thruster plasma oscillations based on the empirical mode decomposition. *Phys. Plasmas*, 12(123506), 2005.

[18]J. Vaudolon, B. Khiar, S. Mazouffre. Time evolution of the electric field in a Hall thruster. *Plasma Sources Sci. Technol.*, 23(022002), 2014.

[19]Yu. B. Esipchuk, A.I. Morozov, G.N. Tilnin, A.V. Trofimov. Plasma oscillations in closed-drift accelerators with an extended acceleration zone. *Zh. Tekh. Fiz.*, 43:1466–1473, 1973.

[20]J. Vaudolon, S. Mazouffre. Indirect determination of the electric field in plasma discharges using laser-induced fluorescence spectroscopy. *Phys. Plasmas*, 21(093505), 2014.